JOM
https://doi.org/10.1007/s11837-024-06852-4

Hybrid Modification of Microstructure and Tensile Properties of A319 Alloy by Heat Treatment and Be Addition

MOSTAFA KARAMOUZ [1,3] and SEYED MOHAMMAD JESMANI[2,4]

1.—Department of Metals, Institute of Science and High Technology and Environmental Sciences, Graduate University of Advanced Technology, Kerman 7631885356, Iran. 2.—Department of Materials and Metallurgical Engineering, National University of Skills (NUS), Tehran 1435761137, Iran. 3.—e-mail: karamouzmostafa@gmail.com. 4.—e-mail: smjesmani@tvu.ac.ir

The microstructure and tensile properties of A319 aluminum alloy were modified by three methods including the addition of three different amounts of beryllium, T4 heat treatment, and a hybrid method of adding 0.06 wt.% Be plus T4 heat treatment. The optimal amount of Be was 0.06 wt.%, which resulted in almost the absence of the β-phase and the best aspect ratio of the α-phase and changed the coarse acicular Si to fibrous Si. However, the T4 heat treatment distributed the phases uniformly, but it could not inhibit the formation of the β-phase. The hybrid method led to the best results since the addition of Be caused the formation of the α-phase, prevented the formation of the β-phase and distributed the phases uniformly. Moreover, the fracture mode in the sample modified by the hybrid method was completely ductile while the other samples exhibited a contribution of brittle fracture to some extent.

INTRODUCTION

Al-Si cast alloys are widely used to produce automobile-related components such as engine parts and power train components[1,2] owing to their outstanding properties such as high specific strength,[3,4] high castability,[5] recyclability,[6] and corrosion resistance.[7] However, the mechanical properties of these alloys directly depend on several factors including composition, the alloying elements, applied heat treatments, melt treatments, and solidification rates.[8] For instance, in the composition factor, iron can dramatically degrade the mechanical properties of A3XX alloys since it forms brittle intermetallic compounds such as β-Al_5FeSi and α-$Al_{15}(Mn, Fe)_3Si$ with the presence of Si.[9,10] The former is acicular or platelet-like and deteriorates the ductility of alloys[11] while the latter exhibits less negative effects.

There are many studies dealing with the modification of A3XX alloys. For example, Srivinas et al.[6] reviewed the effect of the addition of various trace elements such as Mg, Sr, Sc, Cu, Ni, Ti, B, Mn, V, Zr, and Ca, reporting the separate influences of all of these elements on both microstructure and mechanical properties of A319 and A356 alloys. Khalifa et al.[12] used ultrasonication to refine the microstructure of A380 alloy but they could not solve the problem of Fe-intermetallics and Si particles although they refined the grains. Cai et al.[13] applied a short T6 heat treatment on Al-Si-Mg-Mn die-cast alloys and achieved comparable mechanical properties to those that underwent long T6 heat treatment. Vanderluis et al.[14] added Sr to the A319 alloy and at the same time applied long-time stepwise cooling to modify the alloy. Khisheh et al.[15] studied the effect of the T6 heat treatment on fatigue and fracture properties of the A380 aluminum alloy and extended the fatigue life of this alloy used as engine cylinder heads. Emamy et al.[16] tried to refine the microstructure of the A356 alloy by adding Ti, B, and Zr to the melt and found that B exhibited the strongest effect. Qiu et al.[17] modified a near-eutectic Al-Si alloy with various amounts of samarium and found the optimal content of Sm to simultaneously refine primary Si and modify the eutectic mixture. Karamouz et al.[18] added lithium and applied T4 heat treatment to modify the

(Received April 24, 2024; accepted August 19, 2024)

Published online: 09 September 2024

microstructure and mechanical properties of A380 alloy and found that the combination of Li addition and T4 heat treatment could achieve much better results.

However, precautions must be taken to use Be in metallurgical processes, especially during melting and casting operations, which may lead to significant health risks that must be meticulously managed. Beryllium is highly toxic, and exposure to its fumes and dust during melting can lead to severe respiratory issues, including chronic beryllium disease (CBD) or berylliosis. Thus, stringent control measures, including the use of appropriate respiratory protection, adequate ventilation systems, and regular health monitoring of workers, are imperative when handling beryllium-containing materials. These precautions are crucial to prevent inhalation and manage the health risks associated with beryllium exposure in industrial settings.[19]

Therefore, although it appears that the modification of A3XX alloys has been frequently attempted, achieving better results by adding new elements and new methods including hybrid ones is still possible. The present research used a hybrid method, i.e., Be addition and T4 heat treatment, to modify the microstructure and mechanical properties of the A319 alloy and compares the results with those obtained by separate Be addition, the T4 heat treatment, as well as similar studies that were previously published.

MATERIALS AND METHODS

Pure Al (99.87%), Si (99.99%), Cu (99.9%), and Al-8%Fe master alloy were used to prepare A319 alloy in an electrical resistance furnace. The chemical composition of the alloy can be found in Table I. Be was added to the melt using Al-8 wt.% Be master alloys after calculating the exact weight to achieve the required Be amount for each sample. Degassing was performed by pouring dry C_2Cl_6 broken tablets (0.3 wt.% of the molten alloy) followed by adding various amounts of pure Be (0 wt.%, 0.03 wt.%, 0.06 wt.%, and 0.09 wt.%) to the melt at 750°C. Then, immediately after removing the dross, the melt was poured into a ductile iron mold, as shown in Fig. 1a.[18] Also, it is worth noting that the crucible capacity was 1 kg, in which 700 g melt (after removing the dross) was prepared and the mold was kept at room temperature for casting.

Table I. Chemical composition of the A319 alloy

Element	Si	Mg	Fe	Cu	Zn	Ni	Ti	Al
wt.%	6.5	0.08	0.3	3.5	0.2	0.1	0.1	Bal.

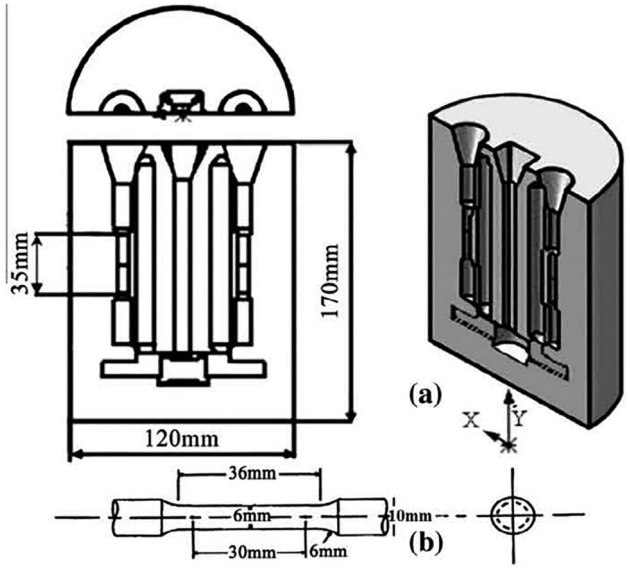

Fig. 1. Schematic illustrations of (a) the cast iron used for casting, (b) the tensile test specimen. This figure is original artwork created by the author using data from Ref. 18.

To find the optimum sample modified by the Be addition, the samples were cut for microstructural studies followed by polishing and etching using Keller's reagent.

For structural studies, section samples were cut from specimens. The cut sections were polished and then etched by Keller's reagent to reveal the structure. The microstructure of the samples was evaluated by an optical microscope, and the micrographs were analyzed using Clemex software. In addition, scanning electron microscopy (SEM-Cam Scan MV2300) was employed for further observations. T4 heat treatment was applied to the optimal sample modified by the Be addition as follows: The A319 alloy underwent solution heat treatment by heating at 500°C for 6 h followed by quenching in water at room temperature, approximately 20–25°C. Then, natural aging was conducted at room temperature for 36 h. Notably, the optimal sample was defined in terms of the microstructural features, i.e., the lack of very harmful β-phase and formation of less harmful α-phase with aspect ratios as close as possible to 1 along with as uniform as possible distribution of the phases formed.

Finally, tensile tests were performed on the specimens (Fig. 1b) of various samples according to the ASTM B557-10 standard using the Universal tensile test machine at a strain rate of 1 mm/min. For each sample, four tests were conducted, and the average value was reported. In addition, the fracture surfaces were evaluated by the above-mentioned SEM to detect the fracture behavior of the samples.

RESULTS AND DISCUSSION

Microstructures

Figure 2 shows the microstructures of various samples. Figure 2a depicts the micrograph of the base A319 alloy or 0 wt.% Be. As can be seen, the base alloy consists of primary aluminum phase, eutectic Si, and β-phase platelets. Other research works[6,20,21] showed that four phases can be detected in this alloy including Al, Si, β intermetallic compounds and Al_2Cu. In this sample, eutectic Si as coarse acicular plates and β-Al_5FeSi intermetallic phase in the form of platelets are dominant in the microstructure. However, the addition of Be led to major differences in the microstructure. As Fig. 2b shows, the addition of 0.03 wt.% Be to the alloy changed the morphology of the phases from acicular to fibrous for Si whereas refined the β intermetallic phase. Nonetheless, the modification continued by adding 0.06 wt.% Be to the base alloy. In this sample, the β intermetallic phase disappeared and instead α-$Al_{15}(Mn, Fe)_3Si$ was formed, which is much better for the mechanical properties since it has a skeletal structure[22] rather than β-Al FeSi with highly faceted platelets possibly up to several millimeters.[23] However, an increase in the content of Be to 0.09 wt.% led to the formation of coarser Si and α-$Al_{15}(Mn, Fe)_3Si$ (Fig. 2d).

To find the optimal sample modified by the Be addition in terms of the microstructural features, the variations of the length and aspect ratio (i.e., the ratio of the length of the precipitate to its width) of various phases were plotted against the Be content of the samples. Figure 3 displays the variations of the length and aspect ratio of the β-phase with the addition of Be. It could be understood that both the length and aspect ratio of this phase decreased with the addition of Be so that the length of the β-phase, which was about 18 μm in the base alloy, decreased to 7.8 μm in the alloy modified by 0.03 wt.% Be. Notably, by increasing the Be content, almost no β-phase (the percentages were very small and close to zero) was formed in those modified by 0.06 and 0.09 wt.% Be in Fig. 3. The Be addition modified the alloy by affecting the nucleation behavior of the β-Al_5FeSi phase. In the A319 alloy system, primary aluminum grains typically crystallize first because of their higher melting point compared to the intermetallic phases. The presence of 0.3% Fe in the alloy can lead to the formation of β-Al_5FeSi, but this typically occurs after the initial formation of primary aluminum grains. The β-Al_5FeSi phase generally forms at a later stage during the solidification process, particularly as part of the eutectic reaction where it solidifies simultaneously with silicon in the interdendritic regions. To clarify, the crystallization of

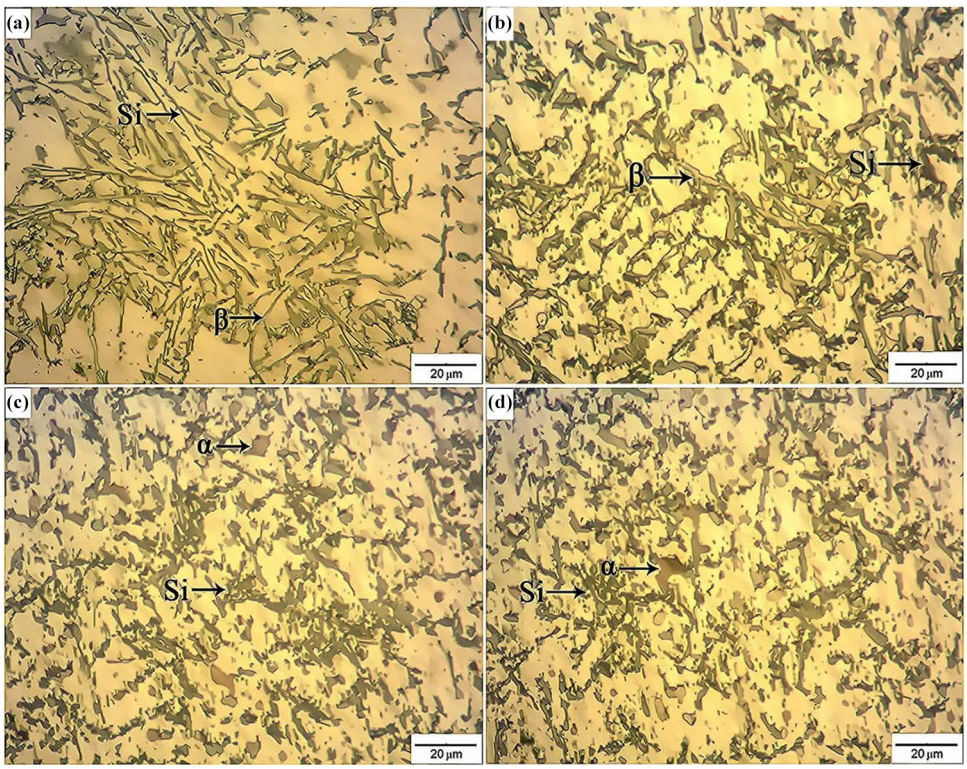

Fig. 2. Optical micrographs of various samples: (a) unmodified A319 base alloy, (b) alloy modified by adding 0.03 wt.% Be, (c) alloy modified by adding 0.06 wt.% Be, (d) alloy modified by adding 0.09 wt.% Be.

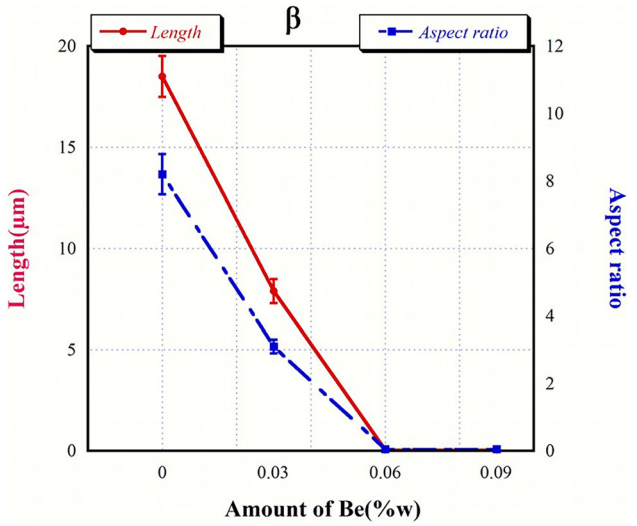

Fig. 3. Variations of the length and aspect ratio of β-phase with various amounts of Be.

primary aluminum grains precedes the formation of β-Al_5FeSi and continues until the eutectic reaction involving α-AlFeSi and silicon phases occurs. This sequence aligns with established solidification behavior for aluminum-silicon alloys with minor Fe additions, as described in sources such as stated by Bäckerud et al.[10] However, comparing these results with the effects of Li on the A380 alloy[18] shows that Li could not effectively modify the microstructure of the A380 alloy since it did not result in the disappearance of β-Al_5FeSi and only refined this phase and changed its dimensions, while Be could completely remove this phase, resulting in the formation of α-$Al_{15}(Mn,Fe)_3Si$. The same trend can be observed for the aspect ratio of the β-phase. Another noteworthy point in Fig. 3 is that the error bars of both the length and aspect ratio data decreased with an increase in the Be content added to the melt. This means that Be addition led to more uniform sizes of the β-phase intermetallic particles.

The variations of the length and aspect ratio of the α-phase and Si can be found in Fig. 4a, b, respectively. This figure proves that no α-phase was formed in the base alloy whereas the Be-modified alloys exhibited the formation of this phase. Moreover, with an increase in the Be content, the length and aspect ratio of the α-phase increased. The aspect ratio of this phase was closer to 1 in the alloy modified by 0.06 wt.% Be, implying that the morphology of this phase is closer to the spherical/equiaxed state. Nonetheless, an opposite trend can be seen in Fig. 4b for Si. The highest aspect ratio (7) and length (24 μm) of Si can be seen in the base alloy, while the lowest values were observed in the sample modified by 0.06 wt.% Be (2 μm and 4.5 μm, respectively). With a further increase in the Be content, these values increased only minorly. Similar to the size of the β-phase intermetallic particles in Fig. 3, the error bars of the Si particles in Fig. 4b decreased with an increase in the Be content of the melt, which implies the more uniform sizes of these particles. However, the error bars of the size of the α-phase particles in Fig. 4a show that the minimum error bar was seen in the sample modified by 0.06 wt.% Be and the other samples exhibited larger error bars. This means that 0.06 wt.% Be had the most uniform size of the α-phase among all Be-modified samples. In brief, with an increase in the Be content, both the length and aspect ratio of the β-phase and Si decreased while the amount of the less harmful α-phase increased. However, since the amount of the β-phase in the samples modified by 0.06 wt.% and 0.09 wt.% Be was almost the same (close to zero) but the length and aspect ratio of Si in the sample modified by 0.06 wt.% be was lower than

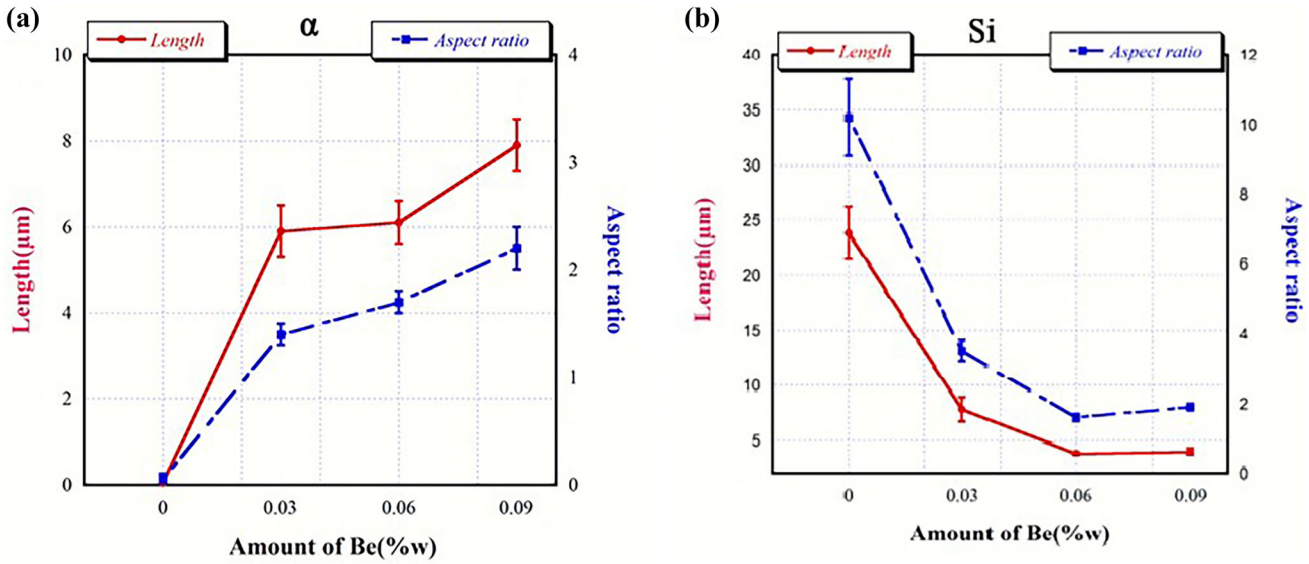

Fig. 4. Variations of the length and aspect ratio of (a) α-phase and (b) Si with various amounts of Be.

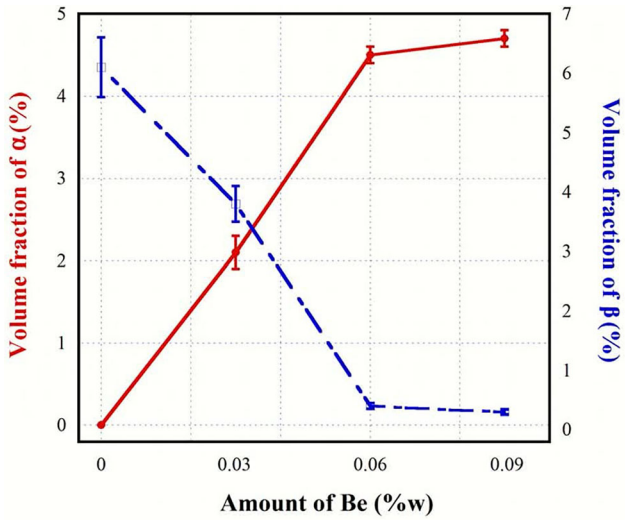

Fig. 5. Variations of volume fractions of α and β with various amounts of Be.

that modified by 0.09 wt.% Be, it could be stated that adding 0.06 wt.% Be led to optimal results among the Be-modified samples in terms of the microstructural features.

As the results in Fig. 5 show, the addition of Be results in a profound change in the iron-bearing compounds forming during solidification. In retrospect, this result might have been anticipated. Be is added in similar amounts to A357 alloy to prevent the formation of the undesirable iron-bearing intermetallic phase $Al_9FeMg_3Si_5$.

Therefore, from Figs. 2, 3, 4 and 5 and the discussion presented, it was confirmed that the addition of 0.06 wt.% Be led to optimal results to modify the microstructure of the A319 alloy. Hence, this sample was chosen for the hybrid modification in the following.

Figure 6 displays the OM micrographs of the samples modified by the T4-heat treatment and the hybrid method. The sample modified by only the T4 heat treatment (Fig. 6a) exhibited only the β-Al_5FeSi intermetallic phase along with eutectic Si particles. Therefore, the major modification of the T4 heat treatment was distributing the phases more uniformly. In addition, some porosities can be found in the microstructure next to the intermetallic phase particles. The hybrid modification of the alloy by the T4 heat treatment plus 0.06 wt.% Be addition (Fig. 6b) led to the best microstructure among the samples since one could see the formation of α-$Al_{15}(Mn, Fe)_3Si$ and Si particles. Also, the distribution of the formed phases in this sample was more uniform throughout the microstructure, and fewer porosities than in the sample modified by the T4 heat treatment could be observed. Then, the hybrid method modified the microstructure more efficiently.

Figure 7 shows the SEM micrographs of the deep-etched samples. Figure 7a shows the SEM micrograph of the base alloy. The presence of long β-Al_5FeSi platelets as well as acicular eutectic Si particles is obvious in this sample. The branches of β-Al_5FeSi can be also detected. However, in the SEM micrograph of the sample modified by 0.06 wt.% Be (i.e., the optimal Be content), the formation of α-$Al_{15}(Mn, Fe)_3Si$, disappearance of β-Al_5FeSi, and change of Si morphology to a fibrous one occurred. The micrograph of the heat-treated alloy in Fig. 7c shows the formation of β-Al_5FeSi but with a lower length than that formed in the unmodified base alloy. Thus, heat treatment could refine the β-phase. The formation of α-$Al_{15}(Mn, Fe)_3Si$ and disappearance of β-Al_5FeSi along with the change of eutectic Si to particles were the result of hybrid modification of the A319 alloy according to Fig. 7d.

Figure 8 shows the volume fractions of α and β phases in unmodified and modified samples. The base alloy exhibited the most unfavorable conditions with the highest β-phase volume (~6.2%) and no detectable α-phase. In contrast, the sample with

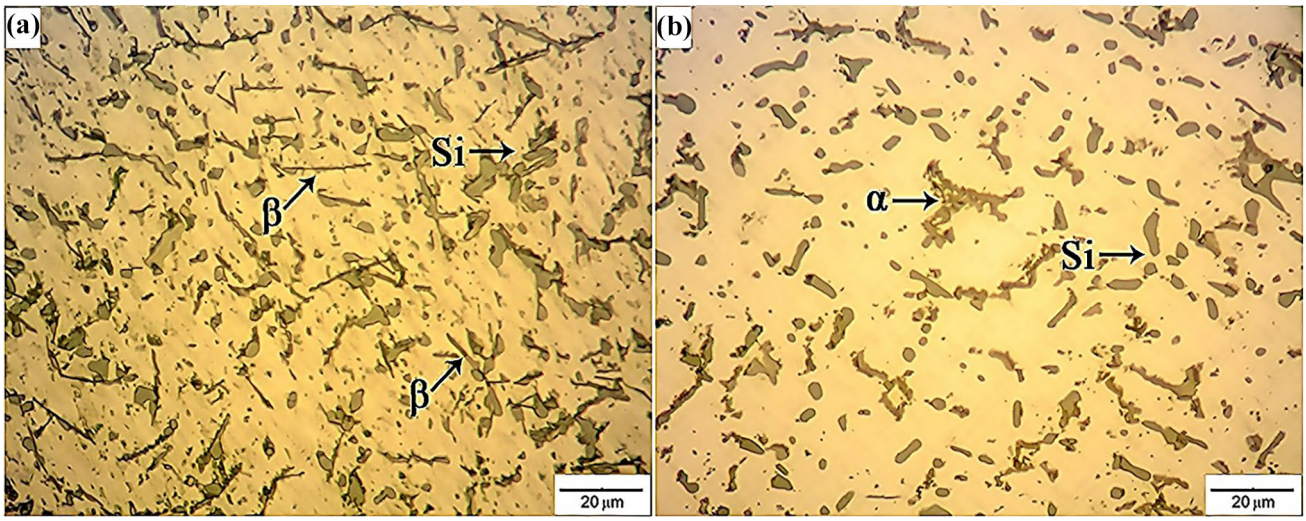

Fig. 6. OM micrographs of (a) alloy modified by the T4 heat treatment, (b) alloy modified by the hybrid method.

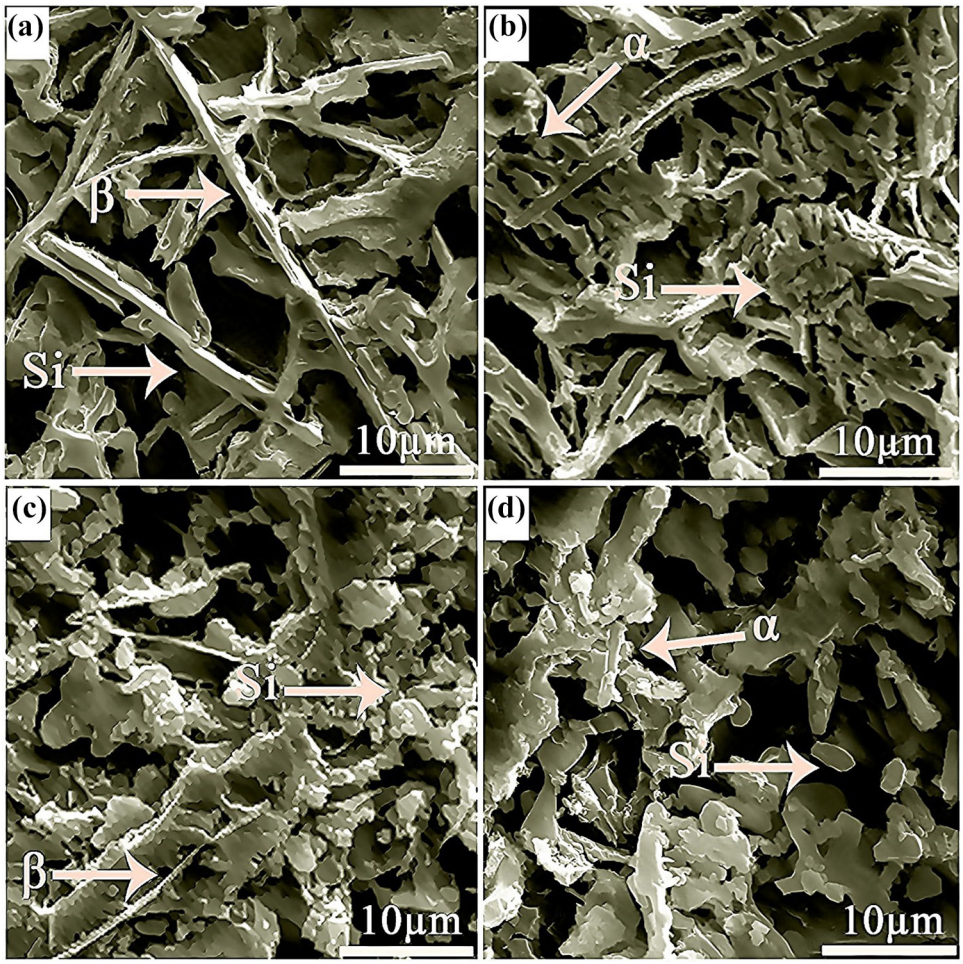

Fig. 7. SEM micrographs of various samples, (a) unmodified A319 base alloy, (b) alloy modified by adding 0.06 wt.% Be, (c) alloy modified by T4 heat treatment, (d) alloy modified by the hybrid method.

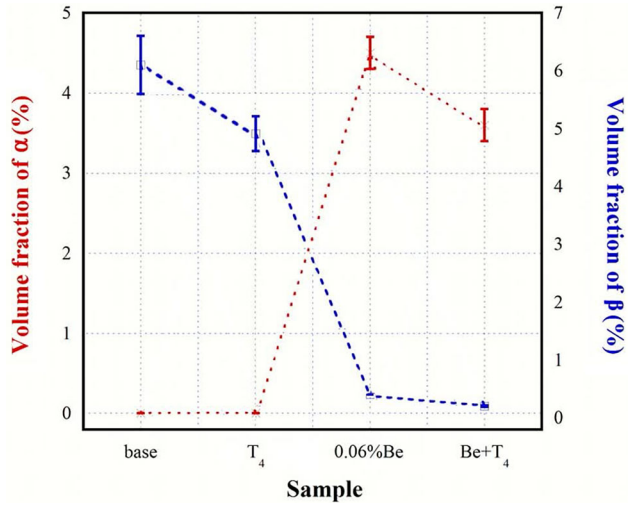

Fig. 8. Variations of volume fractions of α and β in various samples.

0.06 wt.% Be addition displayed the highest α-phase volume (~4.48%) and a minimal β-phase volume (0.09%), observed in the sample modified by the hybrid method. The T4 heat treatment did not induce α-phase formation and resulted in a relatively high β-phase volume. The hybrid method and T4 heat-treated samples showed the smallest error bars, indicating more uniform particle formation caused by these treatments.

Tensile Behavior

Figure 9 shows the tensile strength and elongation percentage of the base alloy, the alloy modified with 0.06 wt.% Be, T4 heat-treated alloy, and alloy modified by the hybrid method. The best results were found in the sample modified by the hybrid method, with a tensile strength of 290 MPa and an elongation percentage of 5.4%. This improvement is due to the addition of Be, which removes detrimental β-phase and forms α-phase, refines eutectic Si, and benefits from T4 heat treatment for better phase distribution. The second-best tensile strength (223 MPa) was in the sample with 0.06 wt.% Be, which also showed improved Si morphology and α-phase formation. However, its elongation (2.5%) was only slightly better than the base alloy (2%). The T4 heat treatment resulted in the second-

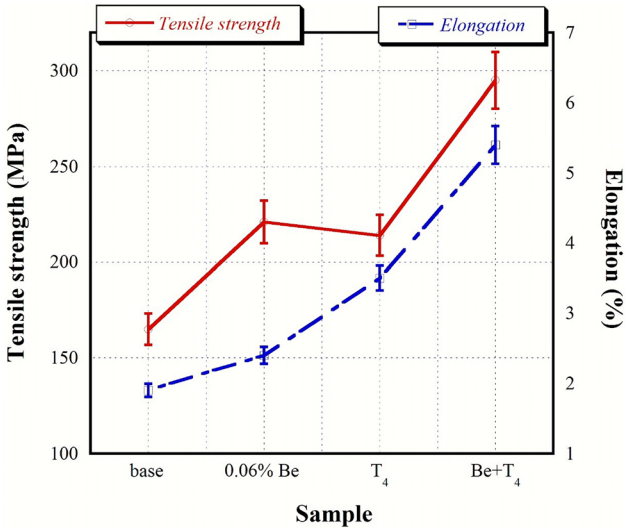

Fig. 9. Variations of tensile strength and elongation percentage in various samples.

highest elongation, likely due to better phase distribution and inhibition of brittle phases, enhancing ductility and elongation as they reduce stress concentration and crack formation.[24,25]

Nonetheless, the T4 heat treatment led to the formation of large porosities,[18,26] which degraded tensile properties compared to the hybrid method. The base alloy had the lowest strength (163 MPa) and elongation percentage (2%) because of the presence of long β-phase platelets and eutectic Si needles, which accumulated in various parts of the microstructure. Comparing these results with the effect of Li and T4 heat treatment on the A380 alloy[18] showed that T4 heat treatment achieved the highest strength and elongation percentage. However, the hybrid method (0.06 wt.% Li + T4 heat treatment) showed the same strength as just adding 0.06 wt.% Li but only slightly improved elongation over the base alloy. Therefore, T4 heat treatment was most effective for modifying the A380 alloy but did not yield the best results for the A319 alloy.

Fractography

Figure 10 displays the fracture surfaces of various samples in this study. Figure 10a depicts the unmodified base alloy. The presence of cleavage planes, as well as large dimples, shows that the fracture mode in this sample was a combination of ductile and brittle fracture, while the brittle fracture was predominant. Moreover, the crack nucleation site can be seen in this sample. The formation of fine dimples along with large dimples is obvious in the fracture surface of the sample modified by the 0.06 wt.% Be addition (Fig. 10b). This shows that the dominant fracture mode in this sample was ductile although several cleavage planes can also be observed. The fracture surface of the sample modified by the T4 heat treatment (Fig. 10c) depicts the presence of cleavage planes as well as porosities, showing the occurrence of brittle fracture. However, a limited number of dimples could be seen, indicating the low contribution of ductile fracture in this sample. Compared with Fig. 10b, the dimples were larger, indicating a decrease in the contribution of ductile fracture by performing the T4 heat treatment. This can be ascribed to the presence of significant porosities in this sample, which amplified the brittle fracture mode and counteracted the uniform distribution of the phases and refinement of the β-phase, leading to increased contribution of the brittle fracture mode. Figure 10d demonstrates the fracture surface of the sample modified by the hybrid method, indicating the presence of fine dimples and the disappearance of porosities in this sample. This shows the occurrence of ductile fracture in this sample. If the size of the dimples is compared, it can be stated that the dimples in the hybrid-method-modified sample were finer than in the other samples, indicating the occurrence of a more ductile fracture in this sample. As stated by other researchers,[27] fine dimples originate from inclusions while large ones are caused by the combination of pores. Therefore, it could be confirmed that no pores were present in the microstructure of the sample modified by the hybrid method. In addition, no crack indication and porosities could be found.

CONCLUSION

The microstructure and tensile properties of A319 alloy were modified by three methods including the addition of three different amounts of beryllium, T4 heat treatment, and a hybrid method of adding 0.06 wt.% Be plus T4 heat treatment. The major results obtained are as follows:

1. All the modification methods exhibited their particular effects. The addition of Be led to the formation of the α-phase and disappearance of the β-phase. T4 heat treatment resulted in a more uniform distribution of the phases. The hybrid method exhibited the best results, i.e., it could modify the microstructure of the A319 base alloy by the formation of the α-phase and inhibiting the formation of the harmful β-phase. Also, it could distribute the phases uniformly.
2. The best values of the tensile strength (290 MPa) and elongation percentage (5.4%) were found in the sample modified by the hybrid method because of the removal of harmful β-phase and formation of the α-phase, the refinement and change of the morphology of eutectic Si, and the uniform distribution caused by the T4 heat treatment.
3. The A319 base alloy exhibited the lowest strength (163 MPa) and elongation percentage (2%) owing to the presence of β-phase platelets with high lengths and aspect ratios and Si needles.

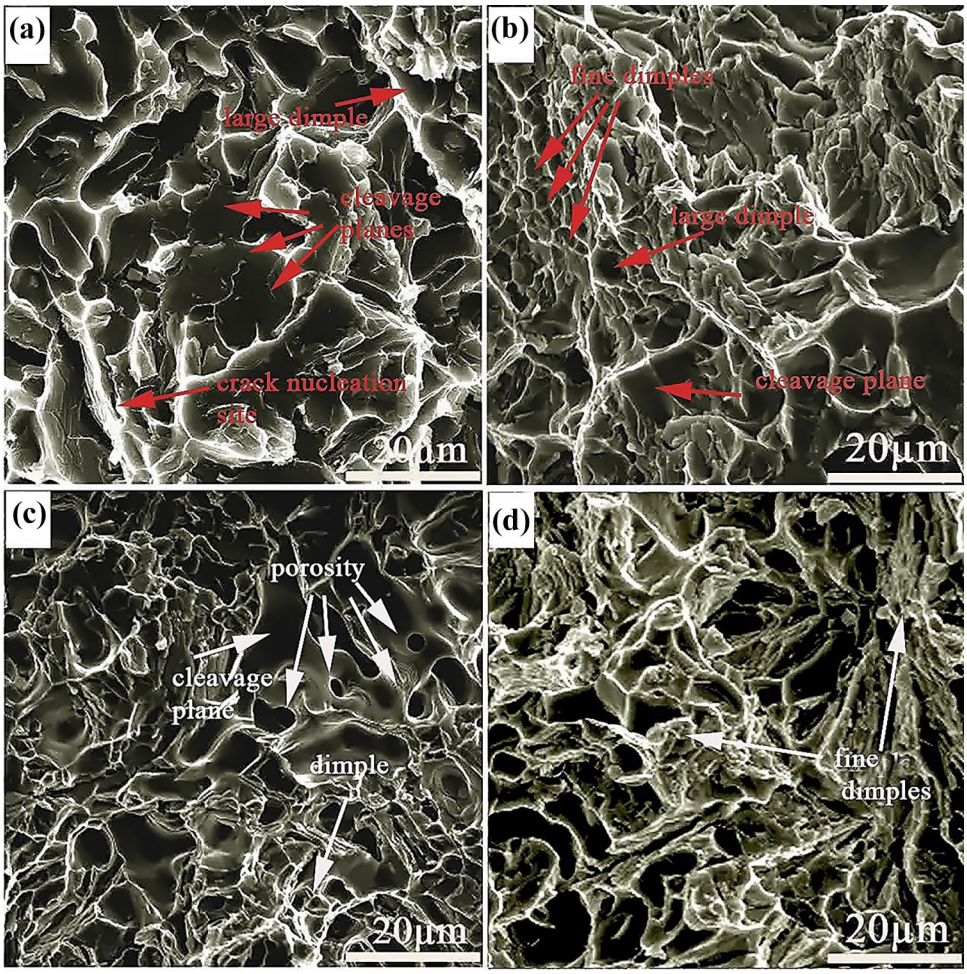

Fig. 10. Fracture surfaces of the samples: (a) unmodified base A319 alloy, (b) alloy modified by adding 0.06 wt.% Be, (c) alloy modified by T4 heat treatment, (d) alloy modified by the hybrid method (T4 + Be addition).

4. The fracture surface of the sample modified by the hybrid method showed the presence of fine dimples and the disappearance of porosities in this sample, which provided the evidence for the occurrence of a completely ductile fracture. However, the other samples showed indications of brittle fracture to some extent.

ACKNOWLEDGEMENT

The authors thank the authorities of Institute of Science and High Technology and Environmental Sciences, Graduate University of Advanced Technology (Kerman, Iran) for providing instruments and facilities to perform this study.

CONFLICT OF INTEREST

The authors declare that they have no conflict of interest

REFERENCES

1. D.K. Yadav and I. Chakrabarty, *Mater. Sci. Eng. A* 791, 139790 (2020).
2. R. Lumley, *JOM* 71, 382 (2019).
3. M. Zamani, L. Morini, L. Ceschini, and S. Seifeddine, *Mater. Sci. Eng. A* 693, 42–50 (2017).
4. S. Adeosun, E. Akpan, S. Balogun, and O. Onoyemi, *JOM* 67, 916–921 (2015).
5. M. De Giovanni, J.A. Kaduk, and P. Srirangam, *JOM* 71, 426 (2019).
6. D. Srinivas, G. MC, P. Hiremath, S. Sharma, M. Shettar, and J. PK, *Cogent Eng* 9, 2007746 (2022).
7. L.F. Gomes, C.L. Kugelmeier, A. Garcia, C.A. Della Rovere, and J.E. Spinelli, *J. Mater. Res. Technol.* 15, 5880 (2021).
8. S. Kori and M. Prabhudev, *Wear* 271, 680 (2011).
9. L.B. Otani, M.M. Matsuo, B.J.M. Freitas, G. Zepon, C.S. Kiminami, W.J. Botta, and C. Bolfarini, *J. Market. Res.* 8, 3539 (2019).
10. L. Bäckerud, G. Chai and J. Tamminen, *Solidification Characteristics of Aluminum Alloys*, (American Foundrymen's Society, 1990).
11. S. Hajas, *Bany Koh Lapok–Ontode–*, 21, 131–134 (1970).
12. W. Khalifa and S. El-Hadad, *Int. J. Metalcast.* 13, 865 (2019).
13. Q. Cai, C.L. Mendis, I.T. Chang, and Z. Fan, *Mater. Sci. Eng. A* 788, 139610 (2020).
14. E. Vandersluis, C. Ravindran, D. Sediako, A. Elsayed, and G. Byczynski, *J. Alloy. Compd.* 792, 240 (2019).
15. S. Khisheh, K. Khalili, M. Azadi, and V.Z. Hendouabadi, *Mater. Chem. Phys.* 264, 124475 (2021).
16. M. Emamy, M. Malekan, A.H. Pourmonshi, and K. Tavighi, *J. Mater. Res.* 32, 3540 (2017).
17. H. Qiu, H. Yan, and Z. Hu, *J. Mater. Res.* 29, 1270 (2014).

18. M. Karamouz, M. Azarbarmas, and M. Emamy, *Mater. Des.* 59, 377 (2014).
19. M.E. Kolanz, *Appl. Occup. Environ. Hyg.* 16, 559 (2001).
20. M. Salleh, M. Omar, J. Syarif, K. Alhawari, and M. Mohammed, *Mater. Des.* 64, 142 (2014).
21. K.-J. Kim and C.-Y. Jeong, *Mater. Trans.* 57, 738 (2016).
22. A.P. Hekimoğlu and M. Çaliş, *Trans. Nonferrous Metals Soc. China*, 31, 2264 (2021).
23. S. Ji, W. Yang, F. Gao, D. Watson, and Z. Fan, *Mater. Sci. Eng. A* 564, 130 (2013).
24. B. Liu, Q. Lei, L. Xie, M. Wang, and Z. Li, *Mater. Des.* 96, 217 (2016).
25. B. Du, Z. Xiao, Y. Qiao, L. Zheng, B. Yu, D. Xu, and L. Sheng, *J. Alloy. Compd.* 775, 990 (2019).
26. S.J. Hirsch, L. Winter, T. Grund, and T. Lampke, *Materials* 15, 2503 (2022).
27. I. Konovalenko, P. Maruschak, J. Brezinová, and J. Brezina, *Materials* 12, 2051 (2019).